

Laser cooling of the vibrational motion of Na₂ combining the effects of zero-width resonances and exceptional points

R. Lefebvre,^{1,2} A. Jaouadi,^{1,3} O. Dulieu,³ and O. Atabek¹

¹*Institut des Sciences Moléculaires d'Orsay, Bâtiment 350, Université Paris-Sud (CNRS), F-91405 Orsay, France*

²*U.F.R. de Physique Fondamentale et Appliquée, Université Pierre et Marie Curie, F-75321 Paris, France*

³*Laboratoire Aimé Cotton, CNRS, Bâtiment 505, Université Paris-Sud, F-91405 Orsay, France*

(Received 20 July 2011; published 24 October 2011)

We propose various scenarios for molecular vibrational cooling combining the effects of two kinds of resonance states occurring during the photodissociation of Na₂ taken as an illustrative example. Such resonances result from an appropriate sampling of laser parameters (wavelength and intensity): (a) For particular choices of intensity and wavelength, two resonance energies can be brought to complete coalescence, with their positions and widths becoming equal and leading to a so-called exceptional point (EP) in the parameter plane. Advantage can be taken from such points for very selective laser-controlled vibrational transfer strategies. (b) For specific intensities, far beyond the perturbation regime, some resonances can have a zero width (infinite lifetime). They are referred to as a zero-width resonance (ZWR) and may be used for vibrational purification purposes. We show how appropriately shaped, experimentally reachable laser pulses, encircling EPs or inducing ZWRs, may be used for a thorough and comprehensive control aiming at population transfer or purification schemes, which, starting from an initial field-free vibrational distribution, ends up in the ground vibrational level.

DOI: [10.1103/PhysRevA.84.043428](https://doi.org/10.1103/PhysRevA.84.043428)

PACS number(s): 37.10.Mn, 33.80.Gj, 37.10.Pq, 42.50.Hz

I. INTRODUCTION

A long-term quest of quantum physicists is the full control of both external and internal degrees of freedom of quantum systems in order to reach the point where their dynamics can be fully driven. The spectacular achievements of laser cooling for more than two decades demonstrate that a broad variety of atoms can be routinely brought to rest in the laboratory framework [1], opening new fields of research such as atom optics [2], quantum degeneracy of dilute gases of weakly interacting ultracold atoms [3], and experimental implementation of quantum bits (qubits) [4]. Due to their rich internal structure, ultracold molecules also offer amazing prospects for ultrahigh-resolution-spectroscopy and precision measurements relevant for testing fundamental theories, cold chemistry, quantum degeneracy of particles with anisotropic interactions, and qubits [5–7]. The main requirement for such studies is the creation of an ultracold molecular sample in a single quantum internal state. This can be fulfilled by slowing down preexisting molecules in a well-defined state using external electric or magnetic fields [8], but such an approach is currently limited to temperatures in the millikelvin range. A powerful alternative approach is to associate ultracold atoms into diatomic molecules with magnetic fields (magnetoassociation, or MA) or with cw lasers (photoassociation, or PA [9]). Regarding the above requirement, both methods present drawbacks. MA leads to the formation of ground-state molecules in very weakly bound ground levels and requires additional steps that are based, for instance, on stimulated Raman adiabatic passage (STIRAP) for transferring the population down to a single strongly bound level, eventually to the lowest one [10–12]. In contrast, PA is efficient in creating samples of tightly bound molecules, but in a distribution of rovibrational levels. It has been demonstrated with ultracold Cs₂ that an additional sequence of shaped laser pulses can transfer most of these molecules in the lowest ground-state vibrational level [13]. It is also worthwhile noting

that in some cases, methods involving PA have even been able to produce specific molecules in their lowest vibrational (RbCs [14]) or rovibrational (KRb [15], LiCs [16]) levels.

In the present work, we propose an alternative to the previous strategies to bring most molecules of an ultracold sample in a single quantum state, based on control with laser pulses. Several theoretical scenarios have been proposed in the past, employing a series of femtosecond shaped pulses [17] or relying on optimal control theory [18,19]. Here we explore yet another strategy, which takes advantage of the unique features arising when a molecule is exposed to a strong laser field. If photodissociation is allowed, the molecular levels become optically induced resonances with complex eigenenergies, which can be of two kinds occurring for suitable choices of the laser parameters (intensity and wavelength). First, a resonance coalescence can be induced, i.e., a degeneracy of their energies, with equality of both the real (position) and the imaginary (width) parts. This circumstance is a very general occurrence in classical as well as quantum physics. The corresponding point in parameter space is called an exceptional point (EP) [20,21]. An important property of exceptional points is that an adiabatic variation of the parameters along a contour encircling an EP induces the transformation of a resonance into a neighboring one [22,23]. We have recently proposed a laser-control scenario for such a transfer in the case of the molecular photodissociation of H₂⁺ [24]. The second type of resonance results from the considerable flexibility offered by the laser parameters governing their widths. More precisely, these widths strictly vanish at particular intensities, for a given wavelength, leading to zero-width resonances (ZWRs). We have previously suggested the use of ZWRs for an isotope separation in a mixture of D₂⁺-H₂⁺ [25], and have more recently shown that efficient purification scenarios can be based on the ZWRs to guide the molecules toward a selected vibrational state [26]. From an experimental point of view, ZWRs have already been exploited for the interpretation of spectral data concerning the predissociation

of IBr [27]. To the best of our knowledge, although EPs have not yet been used in experimental works involving molecular systems, they have recently been directly observed in an open quantum composite of a single atom and a high-Q cavity mode [28].

The present paper proposes to combine both EPs and ZWRs to reach a goal of particular significance: the cooling of a molecule down to its lowest bound vibrational state. It enriches our recent work concerning the laser-controlled cooling of Na₂ [29]. Two strategies are considered, relying either on several laser pulses with each one encircling a single EP at a time and monitoring vibrational transfers between adjacent resonances with $\Delta v = \pm 1$, or a single pulse encircling several EPs between successive resonances allowing cascade transfers with $\Delta v = \pm n$ ($n > 1$). In addition, we show that a purification scenario based on ZWRs can lead to the decay of all resonances, except a given ZWR. A crucial point remains regarding the adiabatic character of the transfer in order to unfold the dynamics by following a single resonance. This requires a laser-pulse duration that exceeds an intrinsic time scale of the system [30,31]. The longer the time, the better is the adiabaticity. On the other hand, a longer pulse duration would induce a less efficient transfer due to dissociation. A compromise has to be found, determined by both the laser-pulse characteristics and the molecular species. In particular, it turns out that a heavier molecule such as Na₂ is by far a better candidate than a lighter one such as H₂⁺. Ultracold Na₂ molecules can be prepared by photoassociation in a distribution of vibrational levels of the lowest (metastable) triplet state, $a^3\Sigma_u^+$ [32]. As for the photodissociation laser, with a wavelength around 560 nm, it can excite the molecule to the continuum of the $(1)^3\Pi_g$ electronic state. As a consequence, all bound levels of the $a^3\Sigma_u^+$ electronic state become resonances. Because the potential energy curve of this state is much flatter than the ground-state potential curve of H₂⁺ studied in Ref. [24], and because the reduced mass is higher by a factor of 20, the density of vibrational levels in Na₂ is large enough to allow the possibility to reach EPs with much weaker laser fields (i.e., 0.3 GW/cm² instead of 0.4 TW/cm² for H₂⁺) [29]. Another favorable circumstance is that an adiabatic following of a Floquet state requires a time of the order of 1000 fs for Na₂, while for H₂⁺, it is 50 fs. Thus the laser parameters necessary for the proposed experiments are much more accessible for Na₂.

The paper is organized as follows: Sec. II gives the elements of the Floquet formalism used in this study. The method to obtain approximate values of the coordinates of exceptional points from a coincidence condition is described in Sec. III, together with the way to determine the loci of ZWRs in the parameter plane. In Sec. IV, we present various transfer scenarios, based either on single or multiple EPs. Finally, in Sec. V, we make use of both ZWRs and an EP to build a transfer scenario, which ends up with the Na₂ molecule in its ground $v = 0$ vibrational state.

II. THE FLOQUET FORMALISM

We use a one-dimensional model involving the spatial nuclear coordinate R , assuming the rotation of the field-aligned molecule is frozen. This approximation is legitimate, as

ultracold molecules created by photoassociation are usually prepared in low rotational levels ($J = 0, 1, 2$). Even if we consider a rotational population peaking at $J = 5$, equivalent to a temperature of 5 K, the shortest rotational period of Na₂ is estimated around 30 ps, which is still longer than the laser-pulse duration of about 13 ps required by the present approach. The model involves only two electronic states, |1⟩ and |2⟩. These labels refer to the lowest triplet $a^3\Sigma_u^+(3^2S + 3^2S)$ and the $(1)^3\Pi_g(3^2S + 3^2P)$ states, respectively. Electronic states are considered to be known in the sense that we give ourselves the electronic energies which serve as potential energies for the nuclear motion. The time-dependent wave function of the system expanded on these two states is written as

$$|\Psi(R, t)\rangle = \xi_1(R, t)|1\rangle + \xi_2(R, t)|2\rangle, \quad (1)$$

where $\xi_1(R, t)$, $\xi_2(R, t)$ are unknown functions describing the field-assisted nuclear dynamics. When the interaction of the molecule with an electromagnetic field with leading frequency ω is described by a periodic time-dependent Hamiltonian, the vector solution of the time-dependent Schrödinger equation (TDSE) can be written as

$$\begin{bmatrix} \xi_1(R, t) \\ \xi_2(R, t) \end{bmatrix} = e^{-iE_F t/\hbar} \begin{bmatrix} \phi_1(R, t) \\ \phi_2(R, t) \end{bmatrix}. \quad (2)$$

E_F is called a quasienergy. According to the Floquet theorem, the functions $\phi_k(R, t)$ ($k = 1, 2$) are periodic in time and can therefore be expanded in a Fourier series,

$$\phi_k(R, t) = \sum_{n=-\infty}^{+\infty} e^{in\omega t} \varphi_{k,n}(R). \quad (3)$$

The elimination of time is then possible by a term-to-term identification because the functions $(2\pi)^{-1/2} e^{in\omega t}$ make up a complete orthonormal set. Within the length-gauge and the long-wavelength approximation for the matter-field coupling, the Fourier components $\varphi_{k,n}(R)$ are given as solutions of the following coupled differential equations [33]:

$$\begin{aligned} [T + V_1(R) + n\hbar\omega - E_F]\varphi_{1,n}(R) - 1/2\mathcal{E}_0\mu(R) \\ \times [\varphi_{2,n-1}(R) + \varphi_{2,n+1}(R)] = 0, \end{aligned} \quad (4)$$

$$\begin{aligned} [T + V_2(R) + n\hbar\omega - E_F]\varphi_{2,n}(R) - 1/2\mathcal{E}_0\mu(R) \\ \times [\varphi_{1,n-1}(R) + \varphi_{1,n+1}(R)] = 0. \end{aligned} \quad (5)$$

$T = [-\hbar^2/(2\mathcal{M})](d^2/dR^2)$ is the usual vibrational kinetic-energy operator and \mathcal{M} is the reduced mass. $V_1(R)$ and $V_2(R)$ are the two *ab initio* Born-Oppenheimer (BO) potentials calculated in [34]. $\mu(R)$ is the electronic transition moment between states |1⟩ and |2⟩ taken from [35]. $\mathcal{E}(t)$ is the laser electric-field amplitude of the form $\mathcal{E}_0 \cos(\omega t)$, with wavelength $\lambda = 2\pi c/\omega$ and intensity $I \propto \mathcal{E}_0^2$. Siegert outgoing wave boundary conditions are imposed to the open channels, resulting in quantized complex quasienergies of the form $E_F = E_R - i\Gamma_R/2$. Γ_R is the resonance width related to its decay rate [33]. Only two channels are needed to describe single-photon processes. The associated functions are $\varphi_{1,0}(R)$ and $\varphi_{2,-1}(R)$. These functions are called diabatic as they are obtained from the coupled equations involving potentials which cross each other. Figure 1 shows the dressed potential-energy curves of Na₂ in this two-channel approximation for a wavelength

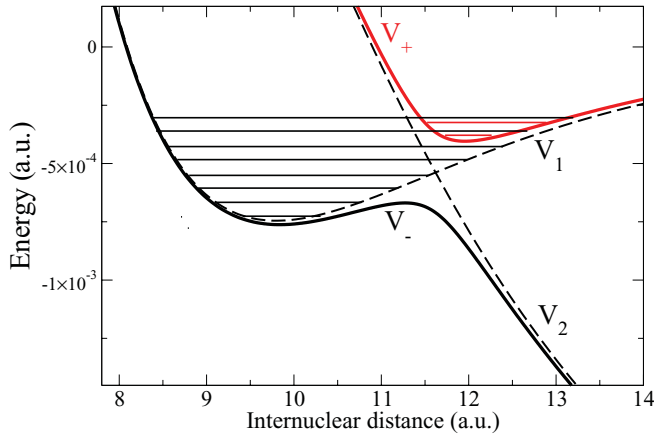


FIG. 1. (Color online) The dressed potential-energy curves describing the photodissociation $a^3\Sigma_u^+ \rightarrow (1)^3\Pi_g$ of Na_2 . The dashed black curves show the potentials $V_1(R)$ (for the $a^3\Sigma_u^+$ state) and $V_2(R)$ [for the $(1)^3\Pi_g$ state], after a shift of $V_2(R)$ by -0.0808 a.u., corresponding to a laser wavelength equal to 564 nm. The solid curves give the adiabatic potentials V_+ (in red) and V_- (in black) after diagonalization of the potential matrix with a field intensity of 0.35×10^9 W/cm 2 . The solid horizontal lines represent the lower field-free vibrational energies (in black) and the energies of the bound states of the upper adiabatic potential (in red).

$\lambda = 564$ nm and an intensity $I = 0.35$ GW/cm 2 . We have solved the coupled equations using a matching technique based on the Fox-Goodwin propagator [36], with exterior complex scaling [37,38]. It is also possible to obtain, through a linear transformation [38], for each value of the R coordinate, the adiabatic channel functions associated with the adiabatic potentials, $V_+(R), V_-(R)$, resulting from the diagonalization of the diabatic potential matrix, including the matter-field interaction.

The width Γ_R resulting from the Floquet theory assumes a cw laser field. Since we consider how the molecule behaves when a pulsed field is applied, it is useful to measure the fraction of nondissociated molecules during a process when the molecule is transported adiabatically from one field-free state to another. This can be done by using the adiabatic Floquet formalism [26,39], with the probability for the molecule to be still in a bound state at time t given by

$$P_{ND}(t) = \exp \left[-\hbar^{-1} \int_0^t \Gamma_R(t') dt' \right]. \quad (6)$$

$\Gamma_R(t')$ is the width of the Floquet quasienergy calculated with the instantaneous field parameters at time t' . The fraction of nondissociated molecules at the end of a pulse of duration t_f is $P_{ND}(t_f)$. Adiabaticity refers here to a transport of a field-free vibrational level on a single Floquet resonance. For a model dealing with EPs, this requires a laser bandwidth narrow enough to avoid resonance mixing between the two-dimensional subspaces built on the pair of resonances participating with the EP and all the others [30,31]. For the energy region of Na_2 that we are considering, $t_f > 850$ fs roughly fulfills such a requirement, on one hand, and validates the frozen rotation assumption, on the other hand.

III. DETERMINATION OF EXCEPTIONAL POINTS AND ZERO-WIDTH RESONANCES

We have previously observed [40] that the Floquet resonances of a molecule undergoing photodissociation fall into two classes: those which are of the Feshbach type (a bound state coupled to a continuum) and those which are essentially of a shape nature (tunneling through or above a barrier). This interpretation is based on the adiabatic potentials shown in Fig. 1, but it is well known that both sets of potentials (diabatic or adiabatic) lead ultimately to the same results if the corresponding equations are properly solved [41]. The resonances belonging to the first class are those with energies increasing as a function of intensity. In strong fields, they finally merge with the levels of the upper adiabatic potential with vanishingly small widths. The others have decreasing energies and increasing widths as the barrier of the lower adiabatic potential is lowered for higher intensities.

An EP is produced when a slight change in the wavelength produces an interchange between the two characters of a resonance. An energy of a bound state of the upper adiabatic potential is always below that of the associated Floquet energy of the Feshbach class. This is due to the way the coupling of such a bound state, with the continuum of states of the lower adiabatic potential, varies with energy. The energy of such a state is necessarily above the region of the avoided adiabatic curve crossing. The coupling of this state with the continuum of the lower adiabatic potential is of a kinetic nature, and depends on the derivatives of both electronic and nuclear wave functions with respect to the internuclear distance [42]. Its highest value is for an energy in the region of the avoided crossing, since this is where there is maximum dependence of the electronic and nuclear wave functions versus R . The consequence is that the level shift from the bound state to the Floquet resonance is positive, explaining the merging from lower energies. This property can be used to get approximate values for the parameters of exceptional points, as it has successfully been applied in the case of H_2^+ [43]. We show in Fig. 2, for Na_2 , how the adiabatic bound energies change with the wavelength when the intensity is arbitrarily small, just enough to produce an avoided crossing between the two potentials. Also shown, as horizontal lines, are the diabatic energies at such an intensity (i.e., the vibrational energies of the field-free molecule). The diagnostic to estimate roughly the wavelength at which an EP is expected is as follows: Consider a crossing between a diabatic energy labeled v with an adiabatic energy with quantum number v_+ occurring for a certain value of the wavelength, say λ_c . If the wavelength is smaller than λ_c , the adiabatic level is below the diabatic energy (which is in fact the Floquet energy at such a field intensity). It is therefore possible for the adiabatic energy to be shifted up in order to merge progressively with the Floquet energy. On the other hand, if λ is larger than λ_c , this merging is no longer possible. In other words, in the first case, we are facing a resonance of Feshbach type, while in the second case, the resonance is of a shape type. Some fine adjustments are needed until the situation of interchange between Feshbach and shape characters is produced. The intensity is determined from the characteristic patterns presented by the energies at an EP [22], which is either a crossing of real parts and an

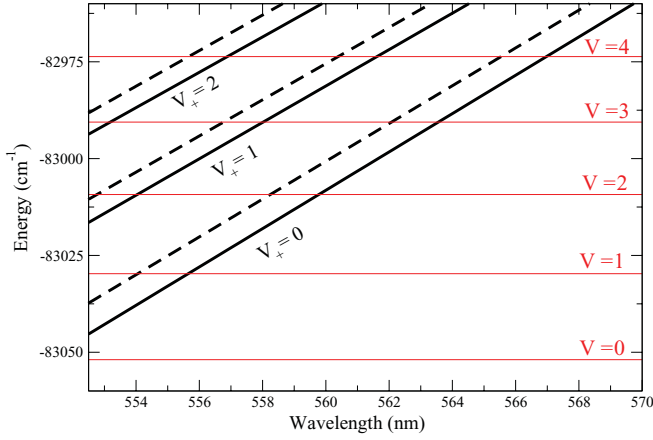


FIG. 2. (Color online) The diabatic energies (as horizontal thin lines labeled by v) and the energies of the upper adiabatic potential at an intensity arbitrarily small to provoke an avoided crossing (solid ascending curves labeled by v_+) as a function of wavelength. The dashed ascending curves represent the energies of the upper adiabatic potential with a phase correction [cf. the quantization rule given in Eq. (8)]. Every crossing between curves of the two families gives an approximate value for the wavelength of an exceptional point. Such a crossing is associated with a change of the character of the resonance state: Feshbach is on the left of the crossing, shape is on the right.

avoided crossing of imaginary parts, or the opposite situation. The multiple crossings between the given diabatic energies v and the successive adiabatic levels $v_+ = 0, 1, 2$, as illustrated in Fig. 2, suggest the existence of several EPs for a given pair of resonances, occurring at different wavelengths. It turns out that this is actually the case, which has important consequences in the laser control of vibrational transfers. In particular, as it will be shown later, when multiple EPs occur in well-organized clusters, cascade-type transfers can be looked for, involving the selective exchange of multiple vibrational quanta, $\Delta v = \pm n (n > 1)$. An example of such clusters has been evidenced in the case of the lighter molecule H_2^+ [43].

As previously shown by Child in the case of predissociation [27], a ZWR corresponds to a coincidence of two kinds of energies. The first kind comprises the so-called “modified diabatic energies.” They obey the semiclassical quantization rule

$$\int_{R_1}^{R_0} k_-(R) dR + \int_{R_0}^{R_d} k_+(R) dR = (\tilde{v} + 1/2)\pi. \quad (7)$$

The members of the second kind are the so-called “modified adiabatic energies” given by the quantization rule

$$\int_{R_2}^{R_d} k_+(R) dR + \chi = (\tilde{v}_+ + 1/2)\pi. \quad (8)$$

\tilde{v} and \tilde{v}_+ are integers. R_1 and R_2 are the left turning points of potentials $V_-(R)$ and $V_+(R)$, respectively. R_0 is the diabatic crossing point. R_d is the right turning point of potential $V_+(R)$. The wave numbers are

$$k_{\pm}(R) = \hbar^{-1} \{2\mu[E - V_{\pm}(R)]\}^{\frac{1}{2}}. \quad (9)$$

E is the energy fulfilling the requirement of quantization rules [Eqs. (7) and (8)]. χ is a phase related to the Landau-Zener parameter [27]. For our purpose, which is to look for

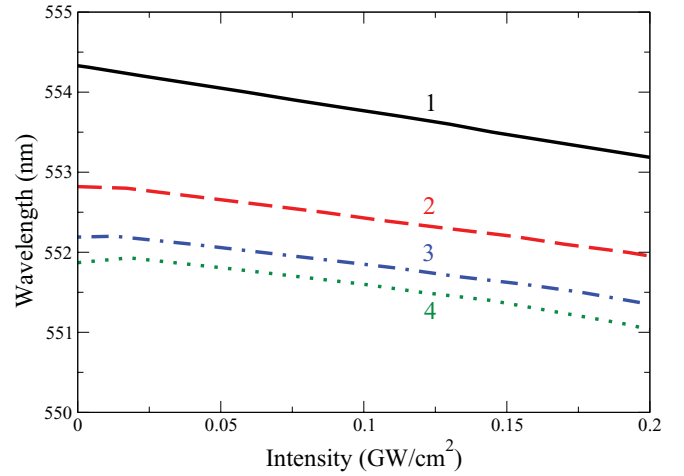


FIG. 3. (Color online) Loci of some ZWRs in the laser parameter plane. The numbers indicate from which field-free state they originate.

coincidences at very small intensities, χ is close to $-\pi/4$. The reason for this choice is that we want to follow the trajectories of the ZWRs in the laser parameter plane when they start from the $I = 0$ axis. We have shown before [44] that ZWRs can occur for arbitrarily small intensities. This is, of course, not to be confused with the trivial vanishing of the width for a zero intensity. In order to determine the associated wavelengths, we examine again Fig. 2 for the phase-corrected adiabatic energies. The effect of χ is far from negligible. As shown by the quantization rule for the “modified adiabatic energies” [Eq. (8)], a value of χ equal to $-\pi/4$ amounts to an upward displacement of the levels approximately equal to one-fourth of the energy separation between adjacent levels. For the vibrational states $v = 1$ to $v = 4$, Fig. 3 gives the loci of ZWRs in the laser parameter plane. Floquet calculations are more and more difficult as the field intensity becomes close to zero because of a possible confusion between naturally decreasing widths of all resonances and strictly zero widths of ZWRs. However, the extrapolation from the ZWR loci toward $I = 0$ turns out to be a good approximation for these ZWRs of the low-field intensity regime. The level $v = 0$ is not shown. The coincidence criterion does not apply as there is no curve-crossing situation. As a full illustration of the Floquet determination of a ZWR resulting from the field-free vibrational state $v = 1$, we indicate, in Fig. 4, the variation of the width as a function of both the field intensity and wavelength. In particular, one observes the locus of the ZWRs in the parameter plane as the bottom of the valley, which starts with natural zero widths at zero-field intensity and displays, through the parameter plane, the quasistraight line of the previous Fig. 3.

IV. COOLING STRATEGIES BASED ON EXCEPTIONAL POINTS

As has previously been shown in theory [22,23], a laser pulse shaped so as to produce a closed contour in the parameter plane which encircles an EP leads to an interchange of the complex energies (both positions and widths) of the resonances involved in the coalescence process, and thus to a vibrational transfer. This property holds even in cases

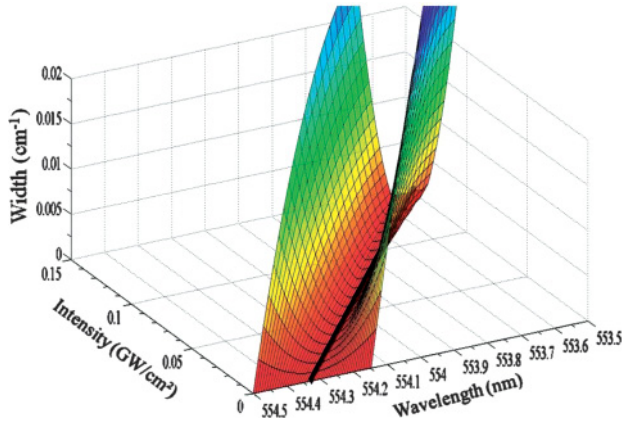


FIG. 4. (Color online) Three-dimensional view of the resonance widths resulting from the field-free vibrational state $v = 1$ as a function of laser intensity and wavelength. The valley of the surface symbolized by the solid black line in the parameter plane corresponds to the locus of the ZWRs, as illustrated in Fig. 3.

where initial and final states are field-free vibrational levels. Advantage has been taken of this situation to build up a workable control scheme by applying a chirped pulse which *selectively* transfers the probability density from one field-free vibrational level to another. As for the *efficiency* of the transfer, it critically depends on the shape or Feshbach nature of the resonances involving large differences in the dissociation rates. Some simple rules emerge [43]. Along a laser loop running clockwise around an EP involving v and $v - 1$, the Feshbach resonance starting from v remains Feshbach and ends up in $v - 1$. The reverse process, i.e., the same loop running counterclockwise but from $v - 1$ to v , also involves Feshbach resonances. On the contrary, the clockwise contour starting from $v - 1$ to end up in v (or its reverse process, i.e., counterclockwise starting from v to end up in $v - 1$) involves shape resonances. The loops of the first category have, of course, to be preferred for better efficiency, as the Feshbach resonances that they involve have much better robustness against photodissociation. This robustness can quantitatively be measured through the nondissociation probability $P_{ND}(t_f)$, at the end of an adiabatically switched laser pulse, as indicated in Eq. (6).

The loops in consideration are of the form

$$I = I_{\max} \sin(\phi/2), \quad \lambda = \lambda_0 + \delta\lambda \sin(\phi), \quad (10)$$

with the phase ϕ taking a set of values between 0 and 2π . The robustness of the method is in relation to the fact that the requirement for the resonance exchange is only to encircle the EP, whatever the precise shape of the loop is. This is compatible with some uncertainty on the EP position, on one hand, and with a possible default to alignment of the molecules, on the other hand. In particular, more accurate BO potentials, including spin-spin interactions, second-order spin-orbit effects, hyperfine structures, and corrections originating from experimental data on the $a^3\Sigma_u^+$, for instance [45], may actually affect the precise position of the EP in the laser parameter plane. But, for the transfer process to occur, the only requirement is that the EP involving v and $v - 1$ is within the laser loop. The flexibility of the loop in terms of

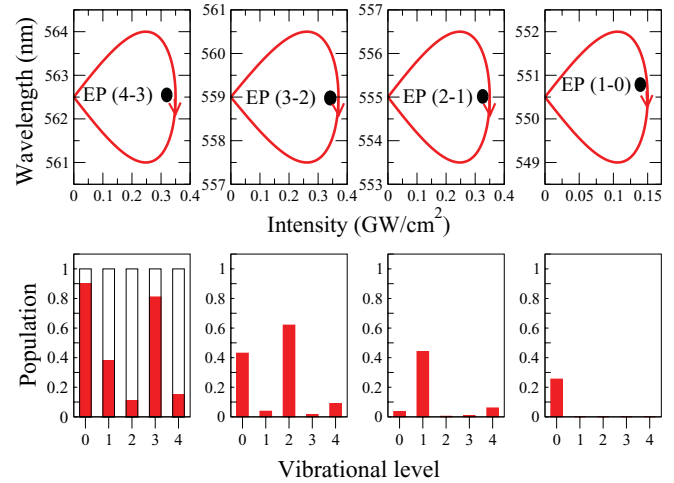


FIG. 5. (Color online) The first row displays the four loops in the laser parameter plane (wavelength vs intensity), each encircling a given EP producing the transfers $4 \rightarrow 3$, $3 \rightarrow 2$, $2 \rightarrow 1$, and $1 \rightarrow 0$. The arrows indicate clockwise contours. The second row displays, in term of histograms, the corresponding nondissociated populations on the vibrational levels $v = 0$ to $v = 4$, with each pulse time being 850 fs. The empty black boxes symbolize the initial uniform distribution of the population.

the chirp parameter $\delta\lambda$ [Eq. (10)] is large enough for such a purpose, while bringing into close proximity the two v and $v - 1$ resonances in consideration. In addition, due to weak interactions between other possible quantum states involved in the dynamics, the degrees of freedom associated with them may safely be considered as frozen during the short laser pulses we are using. As for molecules not aligned along the laser polarization direction, they will experience, for a nominal intensity, a lower radiative interaction in which the effect may be compensated by the extension to higher intensities. In this framework, the relevant laser parameter would be I_{\max} [Eq. (10)].

The goal in molecular vibrational cooling is to reach a single rovibrational state which ultimately is the ground one, when the initial distribution originates from photoassociation and involves a few excited vibrational levels. In the following, for an illustrative purpose, we consider the transitionally cold Na₂ molecule prepared in a distribution of its lowest five vibrational levels, $v = 0$ to 4, with equal probabilities affecting each of them. We refer to and compare the relative merits of two classes of laser-control strategies for obtaining a selective transfer from all vibrational populations to $v = 0$. Such a cooling has, of course, a cost in terms of population loss during the fragmentation process, while the entropy unavoidably flows toward the dissociation continuum. The relative merits concern the efficiency (probability of nondissociated molecules) and the experimental feasibility (shaping and chirping of laser pulses).

The first strategy is based on successive chirped pulses, each encircling a single EP, such as to produce a vibrational transfer between two adjacent resonances, $v + 1$ and v . Figure 5 displays the four pulses each of 850 fs duration expected to produce adiabatic transitions in the energy-gap range of the lowest vibrational levels, with loops in the parameter

plane successively encircling the EPs corresponding to the couples $v = 4 - 3$, $v = 3 - 2$, $v = 2 - 1$, and $v = 1 - 0$. It is important to note that all the loops run clockwise. The residual populations at the end of each pulse are indicated in terms of histograms displayed in the lower row of Fig. 5, where the initial equipartition (as normalized to 1) is symbolized by the empty black boxes. During the first pulse build around EP(4-3), the population exchange concerns $v = 4$ and $v = 3$. More precisely, the population of $v = 4$ is transferred onto $v = 3$ through Feshbach resonances involving low dissociation rates. At the same time, the population of $v = 3$ is transferred onto $v = 4$, but this is done in a much less robust way, as the process goes through shape resonances. The difference in the efficiencies of the two routes is such that at the end of the pulse, the remaining nondissociated population is 80% on $v = 3$ and only 18% on $v = 4$. Of course, during this first pulse, the populations of $v = 0, 1, 2$ are also exposed to dissociation, although they are not directly concerned with transfer mechanisms. As expected, dissociation affects these populations in a way proportional to the width of their corresponding resonances: $v = 2$ is less robust than $v = 1$, which in turn is less robust than $v = 0$. At the end of the first pulse, the population remaining on $v = 2$ is only 12%, while there is still 40% on $v = 1$ and almost 90% on $v = 0$. The purpose of the second pulse is to transfer the vibrational population from $v = 3$ to $v = 2$, using a loop encircling EP(3-2). Here again, the $v = 3$ to $v = 2$ transfer takes advantage of the robust Feshbach resonances, while the $v = 2$ to $v = 3$ reverse process is based on shape resonances. Due to this asymmetry in the exchange mechanism, at the end of the pulse, there remains 62% of the population on $v = 2$, while the nondissociated population is only a few percent on $v = 3$. The populations of $v = 0, 1$, and 4, which are not concerned by the vibrational transfer, are subject to dissociation according to the decay rates of their corresponding resonances. This amounts to 45% of the population remaining on $v = 0$ and only a few percent on $v = 1$ and 4. Similar interpretations hold for the following two pulses aiming in the $v = 2$ to $v = 1$ and the $v = 1$ to $v = 0$ transfers, together with the dissociation of other populations not concerned with the transfer process. As a result of a total radiative exposure time of $4 \times 850 = 3400$ fs, one obtains molecular cooling, with 28% of the initial population nondissociated on $v = 0$ and almost negligible populations on all of the other vibrational levels. In terms of experimental feasibility, we are requiring four differently shaped laser pulses of rather modest maximum intensity of about 0.4 GW/cm^2 , with wavelength chirp amplitudes not exceeding 3%, around 560 nm.

The second strategy takes advantage of the presence of clusters of EPs to control cascade-type transfers from v to $v - n$ (i.e., $\Delta v = n$) using a single chirped pulse encircling several EPs between successive pairs of resonances. In addition to the fact that this requires a simpler experimental arrangement, we expect better efficiency resulting from a shorter total radiative-exposure time. Figure 6 displays a well-organized cluster of three EPs involving the vibrational couples $v = (4 - 3)$, $v = (3 - 2)$, and $v = (2 - 1)$. By “well-organized,” we mean that for a clockwise contour, starting from the highest vibrational level $v = 4$, the occurrence of EPs is ordered from the highest to the lowest v , as time goes on. It is to be

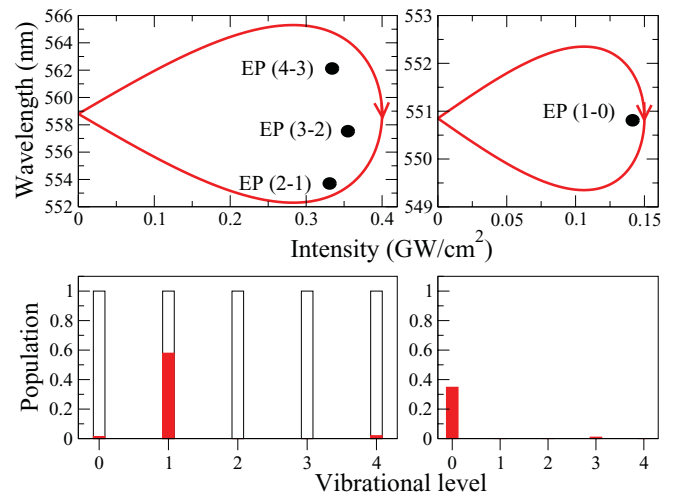


FIG. 6. (Color online) Same information as in Fig. 5, but the first loop encircles three EPs all together.

noted that EP(1-0) is not retained as a member of this cluster, as its characteristic wavelength ($\lambda \simeq 551 \text{ nm}$) and intensity ($I_{\text{max}} = 0.15 \text{ GW/cm}^2$) are much lower compared to those of the cluster ($\lambda \simeq 559 \text{ nm}$ and $I_{\text{max}} = 0.4 \text{ GW/cm}^2$). This is why our strategy is based on a two-pulse process, with one encircling the EP(4-3-2-1) cluster and the other encircling the single EP(1-0). This scheme is more robust than a single pulse encircling all four EPs, with a much larger chirp amplitude and maximum field intensity range. An important issue turns out to be the determination of the total duration of the pulses. With respect to the adiabaticity requirement, two pulses of 850 fs would be convenient. This value is actually the one finally retained for the second pulse encircling the EP(1-0). The analysis of the multiple transfer process for the first pulse is as follows. The clockwise contour, starting from $v = 4$, efficiently and continuously transfers the population from $v = 4$ to $v = 3$ [passing close to EP(4-3)] and then from $v = 2$ to $v = 1$ [passing close to EP(2-1)]. The robustness is in relation to the Feshbach nature of the resonances encountered during these transfers. But, as previously explained for the strategy involving successive pulses, there are also transfers from $v = 3$ to $v = 4$, or $v = 2$ to $v = 3$, and $v = 1$ to $v = 2$, which are unavoidable but fortunately involve shape resonances leading to dissociation. It is precisely these unbalanced population transfers between $\Delta v = +1$ and $\Delta v = -1$ which result in cooling (down, from $v + n$ to v). The important point is to realize that the pulse duration is crucial for avoiding the back transfers (up, from v to $v + n$). In other words, the pulse duration should be long enough for a complete decay of shape resonances responsible for the heating process. A compromise has to be found for the pulse duration, so that it is long enough for the adiabaticity requirement and short enough for the overall efficiency and, of course, for the validity of the frozen rotation approximation. Although we have not proceeded through a full optimization scheme for the most efficient scenario, a duration of 2000 fs for the first pulse seems to satisfy the criteria. As can be seen from Fig. 6, at the end of the first pulse, almost all the nondissociated population is transferred on $v = 1$. The second pulse transfers from $v = 1$ to $v = 0$ with a final efficiency of about 36%. In conclusion,

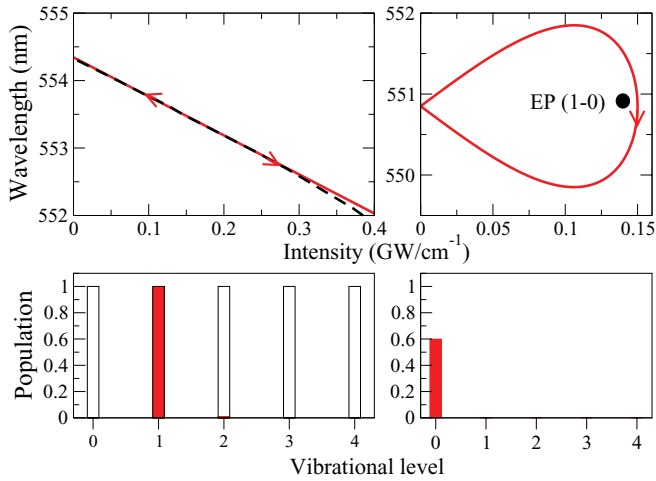


FIG. 7. (Color online) Same information as in Fig. 5. The upper right panel gives the locus of the ZWR corresponding to $v = 1$ in terms of the dashed black line, and the laser loop in terms of the solid red line.

not only is better efficiency achieved, but the proposal rests on a simpler experimental arrangement.

V. COOLING STRATEGY COMBINING ZWRs WITH EPs

Aiming at a much better efficiency, we extend our cooling strategy to a purification scenario, as inspired from our previous works on the use of ZWRs for the laser filtration of a given vibrational level [26]. The leading scheme is to tune laser parameters so as to adiabatically transport a given vibrational level on its ZWR. A laser pulse with these characteristics and of sufficiently long duration will induce the decay of all vibrational populations, except the one which precisely corresponds to the selected ZWR. In this context, one could naively imagine taking advantage of the ZWRs corresponding to $v = 0$. However, this turns out to be more difficult than expected due to the fact that the ZWRs associated with $v = 0$ cannot be simply analyzed within the frame of the semiclassical theory of Sec. III. In particular, an energy matching between “modified diabatic” and “modified adiabatic” levels is out of reach for wavelengths not inducing curve-crossing situations. To go through this caveat, we propose to combine two strategies based on ZWRs and EPs. More precisely, we build a purification scenario to have all the nondissociated molecules left in $v = 1$, followed by the use of an EP(1-0) to finally end with all the surviving molecules in the state $v = 0$. To this end, a laser pulse is designed in such a way as to closely follow the locus of the ZWRs corresponding to $v = 1$ (the one illustrated in Fig. 3). The quasilinear character of this locus allows for an intensity versus wavelength shaping of the form

$$I = a\lambda + b, \quad (11)$$

with the coefficients $a = -0.173$ and $b = 95.8$ to yield I in GW/cm^2 if λ is given in nm. Figure 7 illustrates the agreement reached between this representation and the actual locus of ZWRs for $v = 1$. We take $I = 0.4 \text{ GW}/\text{cm}^2$ as the maximum intensity, which corresponds to $\lambda = 552 \text{ nm}$. The pulse is such

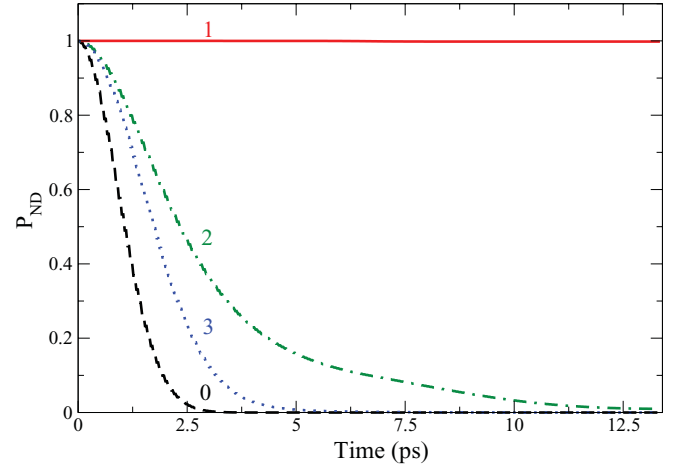


FIG. 8. (Color online) Probabilities for the Na_2 molecule to remain bound in one of its vibrational levels ($v = 0, 1, 2, 3$) as a function of time, when exposed to the laser pulse indicated in Eq. (11) and Fig. 7, with a total duration of 13 ps.

that when this intensity is reached, a backward chirp reduces the intensity to zero, while the wavelength goes back to $\lambda = 554.33 \text{ nm}$. The probability $P_{ND}(t)$ for a molecule to be in a bound state at time t is then calculated for all states from $v = 0$ to $v = 4$, using Eq. (6) and displayed (for the first four states) in Fig. 8. It is interesting to note an almost perfect robustness of $v = 1$ with about 100% of the molecules remaining bound, while a more or less rapid decaying behavior is observed for all other resonances. The purification scheme is complete at about $t_f = 13 \text{ ps}$, with zero final probabilities on all vibrational levels, except $v = 1$, where all of the population has been protected against dissociation.

Since the goal is to have the nondissociated molecules in $v = 0$, we now take advantage of the existence of an EP for the pair (1-0) at $\lambda = 550.85 \text{ nm}$, with intensity $I = 0.1425 \text{ GW}/\text{cm}^2$. With a loop in the parameter plane with $\lambda_0 = 550.85 \text{ nm}$, $\delta\lambda = 1.5 \text{ nm}$, and $I_{\text{max}} = 0.15 \text{ GW}/\text{cm}^2$, the molecules are transferred to $v = 0$, with a probability of about 60%. We emphasize that because the purification (ZWR) step is nondissociative for $v = 1$, this probability actually represents the efficiency of the overall (ZWR + EP) process. With 60% of the initial population of $v = 0$ remaining nondissociated, while all other levels have an almost zero population, this cooling strategy turns out to be the most efficient (and in many cases the easiest experimental method) for molecular cooling.

As cooling is the aim of the strategies involving EPs and ZWRs considered in this work, it is important to show where the entropy goes during the cooling sequence. When referring to ZWRs for purification, the entropy of the system flows through the dissociative decay channels of all vibrational levels v' , except the one v whose population is adiabatically transported on its corresponding ZWR. It is important to note that the population of this specific vibrational state does not increase during the dissociation process; it only decays less than the other populations in such a way that, at the end of the pulse, all other vibrational populations v' are washed out and so purification is obtained with a molecular ensemble in vibrational state v . When referring to EPs, two mechanisms

are operating simultaneously. All vibrational populations are decaying, together with an adiabatic transfer from $v + 1$ to v . At the end of the pulse, the entropy has gone to all decay channels through the radiative coupling with the dissociative electronic state, involving thus both nuclear and electronic degrees of freedom. Depending on the efficiency of the transfer mechanism and the robustness with respect to fragmentation, a certain percentage of its initial population remains on v ($v = 0$, for instance), while all other vibrational populations have been washed out.

Concerning experimental feasibility, we have already mentioned the robustness of the strategy with respect to EPs. The optimization procedure for building up a convenient laser pulse basically involves four parameters: wavelength (frequency), chirp amplitude $\delta\lambda$, maximum intensity I_{\max} , and total pulse duration. Even without an accurate knowledge of the EPs positions, the high flexibility offered by $\delta\lambda$ is such that in all practical situations, a loop encircling the EP in consideration could easily be achieved. For all the examples given in this work, the chirp amplitude is not exceeding 2% of the leading wavelength, which is currently obtainable. To closely follow the ZWR locus (such as the one in Fig. 7, for instance) seems more difficult. But small discrepancies would only affect the efficiency of the overall strategy, not the vibrational purification scheme by itself. The only limitation is to avoid an overlap with a neighboring ZWR locus (as indicated in Fig. 3). For a heavy diatomic like Na_2 , presenting a rather high density of vibrational levels, the maximum laser intensity required for a fine adjustment of close-lying resonances is rather modest (not exceeding 0.5 GW/cm^2) and thus experimentally achievable. The most challenging optimization turns out to be the total laser-pulse duration in order to fulfill the requirements of opposite criteria like frozen rotation approximation and adiabaticity, on one hand, and efficiency (robustness with respect to dissociation), on the other hand. The indications given in this work (i.e., pulse durations of about 1 to 10 ps depending on strategies based on EPs or ZWRs, respectively) may serve as starting points for more realistic search procedures.

VI. CONCLUSION

In conclusion, we have shown how laser-controlled vibrational cooling can be achieved in the photodissociation of molecular systems using a rather simple experimental technique. This is illustrated for the case of Na_2 , with realistic laser parameters leading to appreciable amounts of

non-dissociated molecules in the ground vibrational state. Basically two strategies have been examined based on resonance coalescence: (i) taking advantage of exceptional points for successive vibrational transfers (exchanging single vibrational quantum per laser pulse) and (ii) simultaneous vibrational transfers (exchanging multiple quanta within the duration of a single pulse). But, even more interestingly, we have also examined a strategy based on zero-width resonances, resulting in a vibrational purification scheme, such as to leave (after an appropriately shaped pulse) the molecule in its single, first excited level $v = 1$. A second laser pulse ultimately transfers the population from $v = 1$ to the vibrationless ground state $v = 0$, using an EP associating these two states.

We claim that the proposed scheme can be applied to other molecular species like Cs_2 or Rb_2 , even including rotational degrees of freedom, due to the fact that the wavelength and intensity of the applied electric field give considerable freedom to manipulate the resonance quasienergies originating from a rather high density of vibrational levels. To achieve complete rovibrational cooling, in cases where PA leads to rather high rotational temperatures, our strategies can naturally be extended to pure rotational cooling after the molecule has been prepared in its lowest vibrational level with a distribution of J 's ($v = 0, J$). This can be done by referring to EPs involving the rotational levels in the J manifold of $v = 0$, transferring from level J to $J - 1$. Preliminary calculations show that due to the energy proximity of such levels, very low laser intensities are enough for rotational transfers, which are thus very robust with respect to dissociation. This also implies that adiabatic transfer requirements are fulfilled with even shorter pulse durations (tens of femtoseconds) reinforcing thus the validity of the frozen rotation approximation so far considered in this work. But even simpler in its concept and experimental feasibility is a strategy based on ZWRs. A rovibrational purification scheme could be directly used referring to the locus of ZWRs corresponding to the lowest rovibrational level ($v = J = 0$), with the only requirement being enough accurate laser parameters to avoid the overlapping of neighboring ZWR loci. We are actively pursuing research work in this direction.

ACKNOWLEDGMENTS

R.L. thanks Professor B. I. Ortega for his kind hospitality at Instituto de Ciencias Físicas de Cuernavaca (UNAM) where part of this work has been done. O.A. acknowledges partial support from France-Canada CFQCU Project No. 2010-19. This work is supported in part by Triangle de la Physique.

-
- [1] S. Chu, *Nature (London)* **416**, 206 (2002).
 - [2] S. L. Rolston and W. D. Phillips, *Nature (London)* **416**, 219 (2002).
 - [3] J. R. Anglin and W. Ketterle, *Nature (London)* **416**, 211 (2002).
 - [4] C. Monroe, *Nature (London)* **416**, 238 (2002).
 - [5] K. Burnett, P. S. Julienne, P. D. Lett, E. Tiesinga, and C. J. Williams, *Nature (London)* **416**, 225 (2002).
 - [6] O. Dulieu and C. Gabbanini, *Rep. Prog. Phys.* **72**, 086401 (2009).
 - [7] L. D. Carr and J. Ye, *New J. Phys.* **11**, 055009 (2009).
 - [8] H. L. Bethlem and G. Meijer, *Int. Rev. Phys. Chem.* **22**, 73 (2003).
 - [9] K. M. Jones, E. Tiesinga, P. D. Lett, and P. S. Julienne, *Rev. Mod. Phys.* **78**, 483 (2006).
 - [10] J. G. Danzl, E. Haller, M. Gustavsson, M. J. Mark, R. Hart, N. Bouloufa, O. Dulieu, H. Ritsch, and H.-C. Nägerl, *Science* **321**, 1062 (2008).

- [11] F. Lang, K. Winkler, C. Strauss, R. Grimm and J. Hecker Denschlag, *Phys. Rev. Lett.* **101**, 133005 (2008).
- [12] S. Ospelkaus, A. Peer, K.-K. Ni, J. J. Zirbel, B. Neyenhuis, S. Kotochigova, P. S. Julienne, J. Ye, and D. S. Jin, *Nature Phys.* **4**, 622 (2008).
- [13] M. Viteau, A. Chotia, M. Allegrini, N. Bouloufa, O. Dulieu, D. Comparat, and P. Pillet, *Phys. Rev. A* **79**, 021402 (2009).
- [14] Jeremy M. Sage, Sunil Sainis, Thomas Bergeman, and David DeMille, *Phys. Rev. Lett.* **94**, 203001 (2005).
- [15] S. Ospelkaus, K.-K. Ni, G. Quémener, B. Neyenhuis, D. Wang, M. H. G. de Miranda, J. L. Bohn, J. Ye, and D. S. Jin, *Phys. Rev. Lett.* **104**, 030402 (2010).
- [16] J. Deiglmayr, A. Grochola, M. Repp, K. Mörtlbauer, C. Glück, J. Lange, O. Dulieu, R. Wester, and M. Weidemüller, *Phys. Rev. Lett.* **101**, 133004 (2008).
- [17] A. Bartana, R. Kosloff, and D. J. Tannor, *J. Chem. Phys.* **99**, 196 (1993).
- [18] C. P. Koch, J. P. Palao, R. Kosloff, and F. Masnou-Seeuws, *Phys. Rev. A* **70**, 013402 (2004).
- [19] C. P. Koch, E. Luc-Koenig, and F. Masnou-Seeuws, *Phys. Rev. A* **73**, 033408 (2006).
- [20] T. Kato, *Perturbation Theory of Linear Operators* (Springer, Berlin, 1966).
- [21] W. D. Heiss, *Eur. Phys. J. D* **17**, 1 (1999).
- [22] E. Hernández, A. Jáuregui, and A. Mondragón, *J. Phys. A* **39**, 10087 (2006).
- [23] W. D. Heiss, *Czech. J. Phys.* **54**, 1091 (2004).
- [24] R. Lefebvre, O. Atabek, M. Šindelka, and N. Moiseyev, *Phys. Rev. Lett.* **103**, 123003 (2009).
- [25] O. Atabek, M. Chrysos, and R. Lefebvre, *Phys. Rev. A* **49**, R8 (1994).
- [26] O. Atabek, R. Lefebvre, C. Lefebvre, and T. T. Nguyen-Dang, *Phys. Rev. A* **77**, 043413 (2008).
- [27] M. S. Child, *Mol. Phys.* **32**, 1495 (1976).
- [28] Youngwoon Choi, Sungsam Kang, Sooin Lim, Wookrae Kim, Jung-Ryul Kim, Jai-Hyung Lee, and Kyungwon An, *Phys. Rev. Lett.* **104**, 153601 (2010).
- [29] O. Atabek, R. Lefebvre, M. Lepers, A. Jaouadi, O. Dulieu, and V. Kokooouline, *Phys. Rev. Lett.* **106**, 173002 (2011).
- [30] T. Kato, *J. Phys. Soc. Jpn.* **5**, 435 (1950).
- [31] T. T. Nguyen-Dang, E. Sinelnikov, A. Keller, and O. Atabek, *Phys. Rev. A* **76**, 052118 (2007).
- [32] F. K. Fatemi, K. M. Jones, P. D. Lett, and E. Tiesinga, *Phys. Rev. A* **66**, 053401 (2002).
- [33] O. Atabek, R. Lefebvre, and T. T. Nguyen-Dang, in *Handbook of Numerical Analysis*, edited by C. Le Bris (Elsevier, New York, 2003), Vol. X, p. 745.
- [34] S. Magnier, Ph. Millié, O. Dulieu, and F. Masnou-Seeuws, *J. Chem. Phys.* **98**, 7113 (1993).
- [35] M. Aymar and O. Dulieu, *J. Chem. Phys.* **122**, 204302 (2005).
- [36] L. Fox and E. T. Goodwin, *Philos. Trans. R. Soc.* **245**, 501 (1953).
- [37] N. Moiseyev, *Phys. Rep.* **302**, 212 (1998).
- [38] M. Chrysos, O. Atabek, and R. Lefebvre, *Phys. Rev. A* **48**, 3845 (1993).
- [39] A. Fleischer and N. Moiseyev, *Phys. Rev. A* **72**, 032103 (2005).
- [40] O. Atabek and R. Lefebvre, *J. Phys. Chem. A* **114**, 3031 (2010).
- [41] E. F. van Dishoeck, M. C. van Hemert, A. C. Allison, and A. Dalgarno, *J. Chem. Phys.* **81**, 5709 (1984).
- [42] W. Hobey and A. D. McLachlan, *J. Chem. Phys.* **33**, 1695 (1960).
- [43] R. Lefebvre, A. Jaouadi, and O. Atabek, *Chem. Phys.* (2011), doi: [10.1016/j.chemphys.2011.04.030](https://doi.org/10.1016/j.chemphys.2011.04.030).
- [44] R. Lefebvre and O. Atabek, *Int. J. Quantum Chem.* **109**, 3423 (2009).
- [45] Lus E. E. de Araujo, Jonathan D. Weinstein, Stephen D. Gensemer, Fredrik K. Fatemi, Kevin M. Jones, Paul D. Lett, and Eite Tiesinga, *J. Chem. Phys.* **119**, 2062 (2003).